

1 **Rodent Gut Bacteria Coexisting with an Insect Gut Virus in Parasitic Cysts: Metagenomic  
2 Evidence of Microbial Translocation and Co-adaptation in Spatially-Confined Niches**

3 Amro Ammar <sup>1,2\*</sup>, Vaidhvi Singh <sup>1,2\*</sup>, Sanja Ilic <sup>3</sup>, Fnu Samiksha <sup>7</sup>, Antoinette Marsh <sup>6</sup>, Alex  
4 Rodriguez-Palacios <sup>1,2,4,5</sup>.

5 <sup>1</sup>Division of Gastroenterology and Liver Disease, Case Western Reserve University School of  
6 Medicine, Cleveland, OH 44106, USA.

7 <sup>2</sup>Digestive Health Research Institute, Case Western Reserve University School of Medicine,  
8 Cleveland, OH 44106, USA.

9 <sup>3</sup>Department of Human Sciences, Human Nutrition and Food Microbiology, Ohio State  
10 University, Columbus, OH, USA.

11 <sup>4</sup>Department of Molecular Biology and Microbiology, Case Western Reserve University School  
12 of Medicine, Cleveland, OH 44106, USA.

13 <sup>5</sup>University Hospitals Research and Education Institute, University Hospitals Cleveland Medical  
14 Center Cleveland, OH 44106, USA.

15 <sup>6</sup>The Veterinary Medical Center Diagnostic Parasitology, The Ohio State University College of  
16 Veterinary Medicine Department of Veterinary Preventive Medicine, Columbus, OH, USA.

17 <sup>7</sup>Department of Cancer Biology, Learner Research Institute, Cleveland Clinic, Cleveland, Ohio,  
18 USA.

19

20 **Keywords:** Bacteroidota, *Mythimna unipuncta* granulovirus A, *Hydatigera taeniaeformis*,  
21 cysticercosis, *P. distasonis*, *Klebsiella*, Cavernous fistulous tracts, CAVFT, metacestode

22 **Acknowledgements.** This project was conducted with discretionary funds to support the NIH  
23 study grant R21 DK118373 to A.R.-P., entitled “Identification of pathogenic bacteria in Crohn’s  
24 disease.” We thank Afnan Khan and Brandon Grubb for their scientific contributions.

25 **Corresponding author:** [axr503@case.edu](mailto:axr503@case.edu) (Alex Rodriguez-Palacios)

26 \*co-first authors.

## 27 Abstract

28 In medicine, parasitic cysts or cysticerci (fluid-filled cysts, larval stage of tapeworms) are  
29 believed to be sterile (no bacteria), and therein, the treatment of cysticerci infestations of deep  
30 extra-intestinal tissues (e.g., brain) relies almost exclusively on the use of antiparasitic  
31 medications, and rarely antibiotics. To date, however, it is unclear why common post-treatment  
32 complications include abscessation. This study quantified the microbial composition of parasitic  
33 cyst contents in a higher-order rodent host, using multi-kingdom shotgun metagenomics, to  
34 improve our understanding of gut microbial translocation and adaptation strategies in wild  
35 environments. Analysis was conducted on DNA from two hepatic parasitic cysts (*Hydatigera*  
36 (*Taeenia*) *taeniaeformis*) in an adult vole mouse (*Microtus arvalis*), and from feces, liver, and  
37 peritoneal fluid of three other vole family members living in a vegetable garden in Ohio, USA.  
38 Bacterial metagenomics revealed the presence of gut commensal/opportunistic species, including  
39 *Parabacteroides distasonis*, *Klebsiella variicola*, *Enterococcus faecium*, and *Lactobacillus*  
40 *acidophilus*, inhabiting the cysts. *Parabacteroides distasonis* and other species were also present  
41 outside the cyst in the peritoneal fluid. Remarkably, viral metagenomics revealed various murine  
42 viral species, but unexpectedly, it detected an insect-origin virus from the army moth  
43 (*Pseudaletia/Mythimna unipuncta*) known as *Mythimna unipuncta* granulovirus A (MyunGV-A)  
44 in both cysts, and in one fecal and one peritoneal sample from two different voles, indicating  
45 survival of the insect virus and adaption in voles. Metagenomics also revealed a significantly  
46 lower probability of fungal detection in the cysts compared to other samples (peritoneal fluid,  
47 p<0.05; and feces p<0.05), with single taxon detection in each cyst for *Malassezia* and  
48 *Pseudophaeomoniella oleicola*. The samples with a higher probability of fungi were the  
49 peritoneal fluid. In conclusion, commensal/pathobiont bacterial species can inhabit parasitic  
50 tapeworm cysts, which needs to be considered during therapeutic decisions of cysticerci or other  
51 chronic disease scenarios where immune privileged and spatially restricted ecosystems with  
52 limited nutrients and minimal presence of immune cells could facilitate microbial adaptation,  
53 such as within gut wall cavitating micropathologies in Crohn's disease.

## 54 Introduction

55 The microbial communities, with their diversity and interactions, continue to intrigue  
56 scientists due to the unforeseen complexities of symbiosis in many ecosystems<sup>1,2</sup>, including  
57 spatially-confined niches such as within parasitic cysts. The interplay of microbial populations is  
58 critical in maintaining homeostasis and health in the mammalian gut ecology. Therefore, the  
59 study of these microbial communities could help us determine what influences these dynamic  
60 relationships in restricted ecological niches<sup>3,4</sup>, or the evasion of the host immunity in other  
61 confined biological niches, such as within gut wall-associated cavitating micropathologies in  
62 Crohn's disease<sup>5,6</sup>, which we found to have genomic evidence for niche specific genomic  
63 exchange that could favor silent commensalism and immune evasion<sup>6-9</sup>.

64 The relevance of cysticerci in medicine is associated with the diseases that they may  
65 induce as they travel through the body and stop to enter into their seemingly quiescent cystic  
66 stage, where they become space-occupying masses that gradually develop unnoticed by affected  
67 individuals, and which could drag bacteria on integumentary micro-cavitations, as seen with  
68 electron microscopy on tapeworms<sup>10</sup>, from the gut or ingested foods within the gut as parasitic  
69 larvae migrate. Of immunological interest, such migratory parasites enter in contact with tissues,  
70 triggering host immunity which could presumably stress and drive the selection of microbial  
71 communities that successfully survive evading the immune system. How these communities are  
72 assembled in areas distant from the gut where there is a narrow range of nutrient sources and  
73 stressors, and where there is no physical removal of bacteria by peristalsis remains unknown.

74 Commonly, parasitic tapeworms in domestic animals in the adult forms live in  
75 carnivorous species, which then develop cysts within the peritoneal cavity in intermediate hosts,  
76 including humans, as larva migrate after ingestion and activation within the intestinal tract<sup>11-13</sup>.  
77 *Echinococcus granulosus* and other parasites alike<sup>12</sup>, including *Taenia* and *Hydatigera*, are one  
78 of the many pathogenic parasites that seem to facilitate intricate interactions within their  
79 intermediary hosts during migration at the larva stage<sup>12</sup>. In addition to helping us determine to  
80 what extent the cysts could contain microbial species that may contribute to our understanding of  
81 how to best treat, for instance, brain cysticerci in humans, especially children who are almost  
82 always affected by one cysticercus<sup>14</sup>, the study of parasitic cysts in rodents provides an attractive  
83 model<sup>15</sup> for studying microbial survival and symbiosis away from the gut and its nutrient-rich  
84 dietary and fecal environment.

85 Herein, we report the results from a metagenomics community composition analysis in  
86 various tissue samples from a family of wild voles, one of which was affected with two extra-  
87 hepatic parasitic cysts that resembled the appearance of *Echinococcus granulosus* cysts common  
88 in 80.5% of affected humans<sup>14</sup> (dimensions 10 and 12 mm diameter), but was confirmed as  
89 *Hydatigera* (formerly *Taenia*) in this study. The purpose of this study was to assess and report  
90 the community composition metagenomics analysis of parasitic systems in the context of other  
91 organs (feces, liver, peritoneal fluid) among family members of the vole affected with the cysts  
92 to catalogue the bacterial communities that may translocate within parasitic larval stages, and  
93 thrive outside of the typical gut milieu, in the parasitic cysts.

94

## 95 Methods

96       **Animals and location.** Common voles (*Microtus arvalis*) were located in an  
97 experimental community vegetable garden, in peri-urban Ohio, and trapped as a part of a pest  
98 control program using over-the-counter approved humane mouse traps. Samples were collected  
99 in the field, transferred to the lab, frozen, and processed for DNA extraction. The study included  
100 a total of eleven tissue samples obtained from four different voles. The first vole provided the  
101 two cysts located in its abdominal cavity, anchored on the surface of the liver capsule; no other  
102 samples were collected. For the other three animals, we sampled liver, peritoneal fluid, and  
103 feces. The samples were collected and frozen for metagenomic analysis which accounted for  
104 bacteria, viruses, and fungi.

105       **Identification of the parasitic cysts.** The frozen cystic-like structure and the cyst fluid  
106 DNA samples were sent overnight to the Diagnostic Veterinary Parasitology Laboratory, at the  
107 Veterinary Medical Center, The Ohio State University. The cyst was thawed briefly, extraneous  
108 host tissue removed from the cream/white colored cyst using small forceps and a needle. The  
109 cyst was placed on a microscope, covered with a coverslip and pressure applied to flatten the  
110 structure for photo microscopy. Images were captured using an Olympus BX41 with CellSens  
111 software.

112       **Visualization and anaerobic culture of fluid from the parasitic cysts.** To help  
113 determine whether the cysts were harboring live bacteria, we visualized the liquid in phase  
114 contrast medium using a 1000x magnification, and also cultured<sup>16</sup> the fluid by spread-plating 20  
115 microliters onto a pre-reduced tryptic soy 5% defibrinated sheep blood agar (80% N–10% H–  
116 10% CO<sub>2</sub>, at 37°C; Thermo Fisher Scientific) using a variable-atmosphere anaerobic Whitley  
117 workstation A85 (540 plate capacity; Microbiology International, Inc.) as described<sup>6,9</sup>. Individual  
118 colonies were sub-cultured and purified in the same agar and then immediately identified using  
119 matrix-assisted laser desorption ionization–time of flight [MALDI-TOF] mass spectrometry) and  
120 banked in pre-reduced brain heart infusion broth with 7% dimethyl sulfoxide<sup>6,9</sup>.

121       **DNA extraction and metagenomics.** DNA extraction was conducted using the  
122 DNAeasy Qiagen kit, while the DNA was quantified using the GloMax Plate Reader System  
123 (Promega) using the QuantiFluor® dsDNA System (Promega) chemistry. Samples were  
124 submitted for metagenomic analysis to a third party (CosmoID) which has validated methods and  
125 software<sup>17,18</sup> for library preparation, sequencing and cloud-based computing for data analysis<sup>19</sup>.

126       **Library Prep and Sequencing.** DNA libraries were prepared using the Nextera XT  
127 DNA Library Preparation Kit (Illumina) and IDT Unique Dual Indexes with total DNA input of  
128 1ng. Genomic DNA was fragmented using a proportional amount of Illumina Nextera XT  
129 fragmentation enzyme. Unique dual indexes were added to each sample followed by 12 cycles of  
130 PCR to construct libraries. DNA libraries were purified using AMpure magnetic Beads  
131 (Beckman Coulter) and eluted in QIAGEN EB buffer. DNA libraries were quantified using  
132 Qubit 4 fluorometer and Qubit™ dsDNA HS Assay Kit. Libraries were then sequenced on an  
133 Illumina HiSeq X platform 2x150bp.

**Bioinformatics Analysis and metagenome classification.** The system used utilizes a high-performance data-mining k-mer algorithm that rapidly disambiguates millions of short sequence reads into the discrete genomes engendering the particular sequences. The methodology employed in this study uses the CosmosID-HUB for fast and precise metagenomic analysis of microbiome data<sup>18-20</sup>, incorporating detection capabilities at the strain level across multiple kingdoms, along with antimicrobial resistance/virulence factors (AMR/VF), and functional analysis within a singular processing framework, which has been shown recently to perform well compared to other pipelines<sup>17,18</sup>. Herein, we solely report the microbial community composition since the interpretation of functional data for *Bacteroidota* has some limitations and complexity that we recently determined and which are under investigation<sup>8</sup>. The complete documentation for the analysis<sup>19</sup> is available at <https://docs.cosmosid.com/docs/methods> (accessed March 20, 2024). This analysis platform is powered by three core components, a genBook database, a Kepler algorithm, and machine learning filters. The GenBook is a meticulously curated Multi-Kingdom Reference Database featuring over 180,000 genomes and gene sequences from bacteria, fungi, viruses, phages, and protists. Its curation process is designed to enhance sensitivity by reducing redundancy and ensuring homogeneity, particularly in densely populated clades such as *Staphylococcus aureus*. The database universal curation approach allows for consistent analysis across various sample types within a project, ensuring accuracy through genome quality control and minimizing false positives. The Kepler Algorithm is a patented, k-mer based algorithm that offers efficient and highly accurate profiling. It utilizes unique and shared kmers across the phylogenetic tree for precise near-neighbor placement, ensuring these kmers are phylogenetically stable and do not overlap with mobile genetic elements or the human genome. This approach, coupled with GenBook phylogenetic ontology, permits accurate differentiation down to the strain level. Lastly, the system uses Machine Learning Filters within the analysis pipeline which is enhanced by machine learning algorithms trained on over 10,000 samples, allowing for the distinction between genuine signals and background noise. This maintains high sensitivity and precision, as evidenced by superior F1 scores in benchmarks and community challenges.

162 For metagenomic analysis, whole genome shotgun sequencing data (in fastq or fasta  
163 formats) is used. Paired-end files may be combined for analysis if uploaded simultaneously.  
164 Following sample upload, the CosmosID-HUB automatically processes and generates detailed  
165 reports, including tables and visualizations for genome and gene databases, covering bacteria,  
166 fungi, protists, viruses, respiratory viruses, antimicrobial resistance, and virulence factors, which  
167 are shown in this report. As for performance evaluation, studies have validated CosmosID  
168 leading accuracy and resolution in detection. The system demonstrates exceptional identification  
169 accuracy across all taxonomic levels in benchmark datasets, significantly outperforming other  
170 tools, especially in sub-species and strain-level classification.

171 The metagenomics pipeline has two separable comparators, the first consists of a pre-  
172 computation phase for reference databases and the second is a per-sample computation<sup>19</sup>. The  
173 input to the pre-computation phase are databases of reference genomes, virulence markers and

174 antimicrobial resistance markers that are continuously curated and added to an updated taxon  
175 database. The output of the pre-computational phase is a phylogeny tree of microbes, together  
176 with sets of variable length k-mer fingerprints (biomarkers) uniquely associated with distinct  
177 branches and leaves of the tree.

178 The second per-sample computational phase searches the hundreds of millions of short  
179 sequence reads, or alternatively contigs from draft *de novo* assemblies, against the fingerprint  
180 sets. This query enables the sensitive yet highly precise detection and taxonomic classification of  
181 microbial NGS reads. The resulting statistics are analyzed to return the fine-grain taxonomic and  
182 relative abundance estimates for the microbial NGS datasets. To exclude false positive  
183 identifications the results are filtered using a filtering threshold derived based on internal  
184 statistical scores that are determined by analyzing a large number of diverse metagenomes<sup>19</sup>.

185 **Metacestode DNA extraction and sequencing.**

186 Genomic DNA was extracted using DNeasy Blood & Tissue Kit (Qiagen) following  
187 manufacturer's instructions for tissues with a slight modification. During the proteinase K  
188 digestion, the sample was continuously rotated at 56 C for 45 min. The mitochondrial 12S rRNA  
189 gene region PCR was targeted using 20 to 45 ng of genomic DNA per reaction along with Applied  
190 Biosystem Power SYBR Green PCR Master Mix and previously described primers, Cest F: 5'  
191 AGTCTATGTGCTGCTTAT 3' and Cest R: 5' CCTTGTACGACTTACCT 3'. Oberli et al.,  
192 2023. Cycling consisted of 95C for 2 minutes followed by 50 cycles of 95C for 15 sec, 45C for  
193 30 sec and 60C for 1 min on an Applied Biosystems StepOne Instrument. Control DNA of  
194 *Echinococcus granulosus*, *E. multilocularis* and *Taenia* sp. was provided by Kamilyah R. Miller  
195 (Kansas State University). The amplicon obtained from the cystic structure DNA from 6 different  
196 reactions were pooled and purified using QIAquick PCR Purification Kit spin columns. The  
197 purified product and primers were submitted to Genewiz for DNA sequencing. Two replicate  
198 experiments representing both forward and reverse were used to construct the consensus sequence.  
199 The 176 base pair DNA sequence was compared to published sequences using a nucleotide Blastn  
200 search (ncbi.nlm.nih.gov). The resulting DNA sequence was submitted to GenBank accession  
201 PP477764.

202 **Statistics.** This report is primarily descriptive because the number of animals and  
203 samples tested were limited. Univariate analysis of metagenomic community composition and  
204 frequency statistics (presence/absence) for species of interest across the samples<sup>21</sup> was conducted  
205 to determine if findings were random or significantly different from random. For this purpose,  
206 we used Fisher's exact, or Chi-square statistics using GraphPad (v10.2.1) depending on the  
207 number of observations in each cell in a 2xn tables. Statistical significance for expected vs  
208 observed was held at p<0.05.

209 **Data availability.** The metagenomic sequences and fastq files have been deposited in  
210 NCBI GenBank under the BioProject number PRJNA1053337. Entitled 'gut microbiome that  
211 evades host immunity in wild rodents (vole) and parasitic cysts', this project has 11 associated  
212 BioSamples and Sequence Read Archive (SRA) numbers for sharing with the scientific

213 community under submission SUB14073752, and accessions SRR27223102 through  
214 SRR27223112, scheduled for release on April 18, 2024.

215

## 216 **Results**

217 **Nucleotide sequence analysis of metcestode reveals *Hydatigera taeniaeformis*.** An  
218 overview of the cysts and fecal, peritoneal fluid and liver samples, collected from 4 mice, and  
219 processed in this study can be found in **Figures 1A-D**. Although initial environmental assumptions  
220 suggested that *Echinococcus granulosus* was the most likely parasite (e.g., the presence of coyotes  
221 and other carnivores in the farm where the vegetable garden was implemented), DNA  
222 amplification and sanger sequencing results revealed the parasite metacestode was *Hydatigera*  
223 *taeniaeformis*, which forms a strobilocerus as its metacestode stage in the intermediate rodent host.  
224 The NCBI Blastn search showed the greatest percent identity (99%) to *Hydatigera* sp. (Genbank  
225 LC008533.1). Microscopic examination of the parasite confirmed that the segmentation patterns  
226 observed on the surface of the organism are suggestive of an immature strobilocercus metacestode  
227 stage which was discernable on the photomicrographs using the magnification and dorsal ventral  
228 flattening of the cyst. The lack of hooks and size suggests that this cyst-like structure is an  
229 immature strobilocercus.

230 **Visualization and cultivation of fluid yielded *Enterococcus faecium*.** Of interest, we  
231 were able to visualize the presence of highly mobile bacterial-like structures in the fluid  
232 examined under contrast phase microscopy and visualized a complex array of gram-positive and  
233 gram-negative bacteria. However, also of interest, cultivation of the cysticercus fluid only  
234 revealed the presence of pure colonies of *Enterococcus faecium*, which were identified using  
235 Maldi-Toff. Although gram-staining of biological samples do not resemble the textbook gram-  
236 stain description of microbes isolated on agar surfaces, the isolation of pure *Enterococcus* on the  
237 agar (typically gram-positive cocci), and not of other bacteria, indicates that the cohabitation of  
238 multiple bacteria in a spatially-confined nutrient-depleted biological niches, such as the cysts,  
239 could be rendering *Enterococcus* species more symbiotic with other community members,  
240 instead of being inhibitory once it is growing on an artificial nutrient rich medium such as 5%  
241 sheep blood TSA plates as we previously documented for a fecal *Enterococcus* strain against a  
242 co-inhabitant *Lactobacillus* in the intestinal tract in a mouse model of Crohn's disease<sup>22</sup>.  
243 Metagenomic analyses where therein pursued to better characterize the non-cultivable species in  
244 the cysts.

245 **Metagenomics of the cystic fluid revealed gut commensal/opportunistic bacteria.**  
246 Metagenomic analysis revealed a relatively simple bacterial community inside the two cysts,  
247 demonstrating that these symbiotic bacteria could avoid the immune system and flourish over  
248 time in a nutrient-depleted lesion. At the species level, *Klebsiella variicola* comprised 18.34%  
249 and 35.48% of the total bacterial population in cysts 1 and 2, respectively, followed by  
250 *Enterococcus faecium* in cyst 2 (32.59%). *K. variicola* was also highly abundant in the peritoneal  
251 fluid samples of vole 2 (33.34%), vole 3 (39.86%), and vole 4 (74.9%), and feces samples of

252 vole 2 (29.66%) and vole 4 (37.96%). In contrast, the vole 3 liver was entirely inhabited by  
253 *Propionibacteriaceae*, which only constituted 8.95% of cyst 1 (**Figures 2A-B**).

254 *Bacteroidales* amassed an abundance of 23.29% in cyst 1 and 10.28% in cyst 2. At the  
255 species level, the cysts 1 and 2 had a very comparable abundance of *Parabacteroides distasonis*  
256 with 9.08% and 9.88%, respectively. The analysis of peritoneal fluid revealed *P. distasonis* as  
257 the most prevalent bacteria (42.39%) in vole 2, and as a highly abundant bacteria in vole 3  
258 (9.36%). Of note, vole 3 was inhabited by *Quadrisphaera* sp. DD2A (44.69%). The latter finding  
259 is of notoriety, since the DNA of fecal samples in this study did not reveal a large number of  
260 bacterial taxonomic units, as expected from other studies we have conducted in human  
261 colonoscopy content and in mice<sup>7,22</sup>, with the same methodology, or using 16S rRNA  
262 microbiome studies<sup>23,24</sup>. This finding could be attributed to completely different gut microbiome  
263 in these wild animals who inhabit subterranean environments and have different diets. Repeated  
264 testing confirmed the limited detection of OTUs in feces on this study.

265 **Identification of insect virus outside its natural habitat.** Our metagenomic analysis  
266 reports, for the first time, the presence of a virus, *Mythimna unipuncta* granulovirus A  
267 (MyunGV-A), a virus adapted to the insect armyworm *Mythimna unipuncta*<sup>25</sup> (which feeds on  
268 crops, including corn<sup>26</sup>), detected outside of its natural insect habitat, inside parasitic cysts within  
269 voles. MyunGV-A naturally infects and replicates within the larvae of the armyworm moth,  
270 *Mythimna unipuncta*, primarily within the cells of the midgut epithelium.

271 Our study identifies the presence of MyunGV-A in high abundance, suggesting that the virus  
272 may be thriving inside the cyst through cohabitation with the bacteria, and the absence of other  
273 viruses that were identified in the liver, peritoneum and feces of the other voles. MyunGV-A was  
274 found to be the only viral species in both cysts, while it was combined with Human  
275 mastadenovirus C in vole 2 peritoneal fluid (61.19%; **Figures 3A-B**). In vole 4 peritoneal fluid  
276 and vole 2 feces, MyunGV-A relative abundance was 100%, since no other viruses were  
277 detected. The liver samples were mostly inhabited by Moloney murine sarcoma virus and Murine  
278 osteosarcoma virus, which are expected infectious viruses of rodents. In the peritoneal fluid of  
279 vole 3, Abelson murine leukemia virus was the most prevalent (51.19%), followed by MyunGV-  
280 A (31.72%). This discovery indicates that MyunGV-A has probably adapted to voles, the  
281 parasite, or to the gut microbiome of mice, or that the microbiome provides metabolites that  
282 enable the virus to colonize other species (mouse or hydatygera), raising questions about the role  
283 of newly adapted, or transiently infecting baculoviruses in rodents and the implications for both  
284 the parasite and its mammalian host.

285 **Metagenomics suggests lower probability of fungal detection in the cysts.** A binary  
286 analysis of the presence or absence of fungal DNA in the samples, regardless of the species  
287 identified, revealed that the animals had a significantly lower probability of fungal detection in  
288 the cysts compared to other samples (peritoneal fluid,  $p < 0.05$ ; and feces  $p < 0.05$ ), with single  
289 taxon detection in each cyst for *Malassezia*, and *Pseudophaeomoniella oleicola*. Of interest, the  
290 samples with higher probability of fungal taxa were the peritoneal fluids.

291

292

293 **Discussion**

294 Herein, we report the results from a metagenomics community composition analysis in  
295 various tissue samples from a family of wild voles, one of which was affected with two extra-  
296 hepatic tapeworm cysts. The tapeworm identified, *H. taeniaeformis*, is widely abundant  
297 globally<sup>27</sup>. Like other tapeworms, this parasite has been documented in a variety of mammals,  
298 primarily infecting cats and other feline species<sup>28</sup> (**Figure 4A**). *H. taeniaeformis* typically infects  
299 felines, having rodents serve as the primary intermediate host for the larval form,  
300 *Strobilocercus*<sup>29,30</sup>.

301 From a microbiome perspective, it is well known that tapeworms affect the gut  
302 microbiome in humans and animals<sup>15,31-33</sup>, they produce secretory molecules which affect the gut  
303 microbiota<sup>34</sup>, and that the infestation promotes the production of immunoglobulins (IgG, IgG1,  
304 IgG2a, IgG2b, IgG3 and IgM) against gut commensals that correlate with increase or decrease in  
305 the feces<sup>15</sup>. Despite this knowledge, little is known about the microbiome features of the cystic  
306 structures of tapeworm larva or other migratory parasites and the potential they may have to  
307 cause local infections. In our study, the identification of bacteria inside the parasitic peri-hepatic  
308 cysts, opens new possibilities for understanding the complicated interplay of viruses, parasites,  
309 and bacteria in the peritoneal cavity of mice.

310 From an ecological perspective, the unanticipated discovery of *Mythimna unipuncta*  
311 granulovirus A (MyunGV-A), commonly a lepidopteran-specific baculovirus, in addition to a  
312 community of bacteria such as *Lactobacillus acidophilus*, *Enterococcus faecium*, *Bacteroidales*,  
313 and *Klebsiella variicola*, inside *H. taeniaeformis* cysts in wild voles challenges conventional  
314 theories of host-virus specificity and microbial dynamics in ecosystems. Although we did not  
315 verify the presence of viruses with cultivation methods or electron microscopy visualization, the  
316 presence of MyunGV-A is intriguing because Baculoviruses, such as MyunGV-A, use receptors  
317 on gut cells of their insect hosts to enable the virus entry, reproduction, and dissemination within  
318 the insect cells<sup>35,36</sup>. The gastrointestinal system of voles, which is normally a reservoir for a diverse  
319 range of commensal bacteria<sup>37,38</sup> could serve as a suitable environment for MyunGV-A survival  
320 and likely replication which we did not visualize<sup>39</sup> or quantify<sup>40</sup>. It is unclear if the virus interacts  
321 with the strobilocercus microbiota, potentially aiding the survival of the community within the  
322 parasite in the mammalian host. If it is not adaptation with replication, another possibility to  
323 observe the infection of the mouse could be through dietary acquisition, in which voles consume  
324 MyunGV-A-carrying insects and temporarily allow the virus to replicate, until the host clears the  
325 viral infection. Although the virus does not reproduce within the vole digestive tract, it is possible  
326 that it could survive in the gastrointestinal environment, if the virus symbiosis takes place with  
327 bacteria, which has not been reported in MyunGV-A viral laboratory strains. Additionally, the  
328 virus and bacteria could enter the systemic circulation via breaks in the mucosal surfaces of the  
329 digestive tract of the voles, resulting in broad translocation and colonization throughout the  
330 peritoneal cavity. The specificity of these viruses is highlighted by their successful usage as  
331 biopesticides<sup>41,42</sup>, which is due to their inability to cross species and infect non-target mammals.

332 Therefore, the existence of MyunGV-A within the rodent tapeworm larval cysts needs further  
333 examination before considering this presumed co-adaptation in migratory parasites as a strategy  
334 for non-traditional viral transmission and survival mechanisms outside the insect gut.

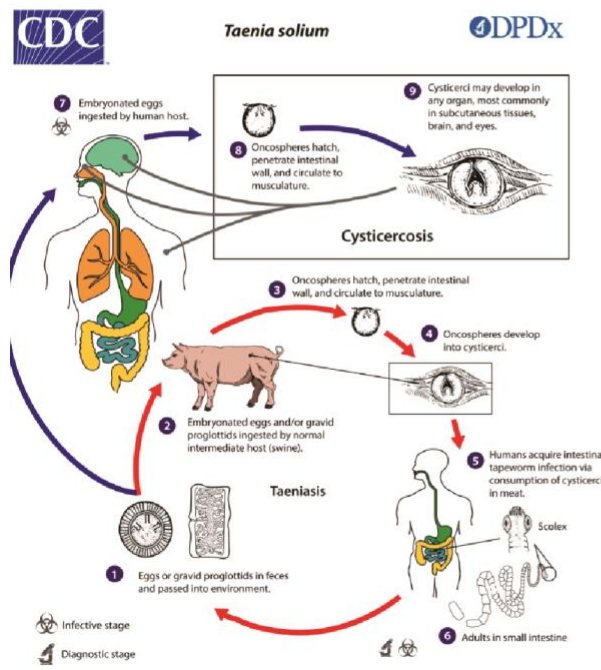
335 The findings also complement the results from a recent study where parasitic tapeworms  
336 of domestic animals in China showed a highly variable virome, but did not identify MyunGV-A  
337 in adult parasites<sup>43</sup> which indicated several possibilities and theories for future testing (**Figure 4B**).  
338 Those theories include that adult tapeworm of domestic animals do not carry MyunGV-A or that  
339 there are virome differences in China vs USA with China not having MyunGV-A, or that  
340 MyunGV-A is likely associated with the gut microbiome of wild voles locally in Ohio being also  
341 independent of the viral load of adult tapeworms.

342 In conclusion, our findings revealed a simplified microbial community within the parasitic  
343 cysts of wild rodents, which contained gut commensals (*P. distasonis*) and an unexpected insect  
344 virus, which thrive reproducibly and independently in spatially-restricted niches, away from the  
345 gut, devoid of host-nutrient availability from ingested food or gut ingesta. Metacestodes represent  
346 a unique model of bacterial community evasion of the immune system and survival in a host-  
347 nutrient-deprived, parasite-acquired environment. This study provides a new perspective on the  
348 understanding of bacterial communities in migratory tapeworms and in dysbiosis associated with  
349 chronic intestinal diseases where spatially-restricted cavitating micro niches develop and could  
350 perpetuate inflammation through symbiotic mechanisms. Such a scenario is in Crohn's disease,  
351 where recently we discovered that *P. distasonis* predisposes susceptible hosts to inflammation  
352 driven by succinate (*P. distasonis* metabolite)<sup>7</sup>, which increases cytotoxicity of immune cells to  
353 co-habiting *Escherichia coli*. Our study could help identify revised strategies for the treatment of  
354 clinical cysticercosis and the potential benefits of adding antibiotics.

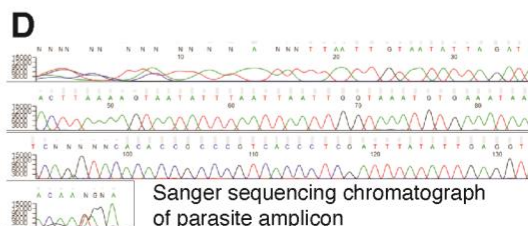
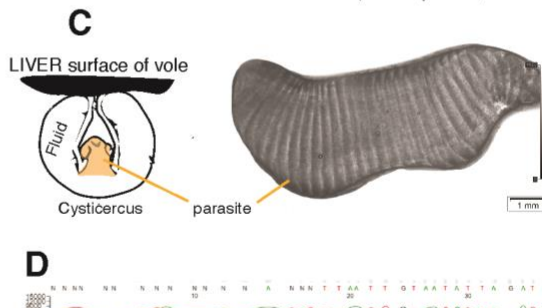
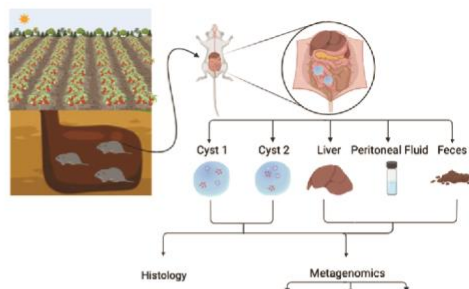
355

356

**A** Overview of life cycle that precedes extra-intestinal formation of cisticerci from *Taenia solium* in humans



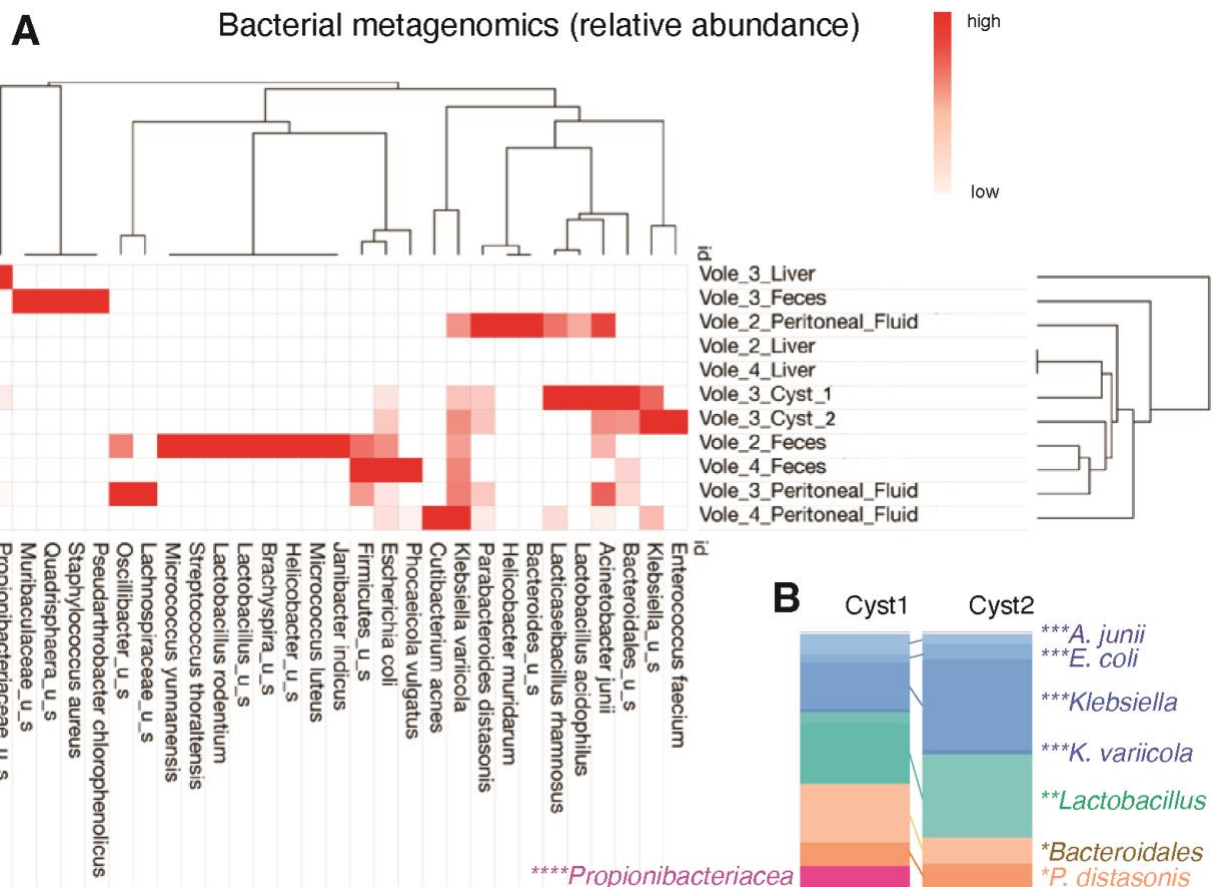
**B** Overview of study of cisticerci in wild voles, this study



357

358 **Figure 1. Overview of family of voles in this study and identification of the hepatic parasitic**  
 359 **cyst as the larval stage of *Hydatigera taeniaeformis* tapeworm. A)** Contextualization of the clinical and ecological relevance of human cysticercosis, exemplified with *Taenia solium*. (CDC public domain image). **B)** Samples collected from the voles in this report. **C)** Schematic of origin of samples within metacestode (parasitic-cystic structure) for analysis and photomicrograph, illustrating distinctive microscopic segmentation of the parasite as indicative of an immature strobilocerus metacestode. Not detailed the parasite lacks visualized hooks and the overall size suggests that this cyst-like structure is an immature strobilocerus. **D)** Chromatogram after Sanger sequencing used for tapeworm identification as *Hydatigera taeniaeformis* illustrates pure DNA in the cyst samples tested in this study.

360

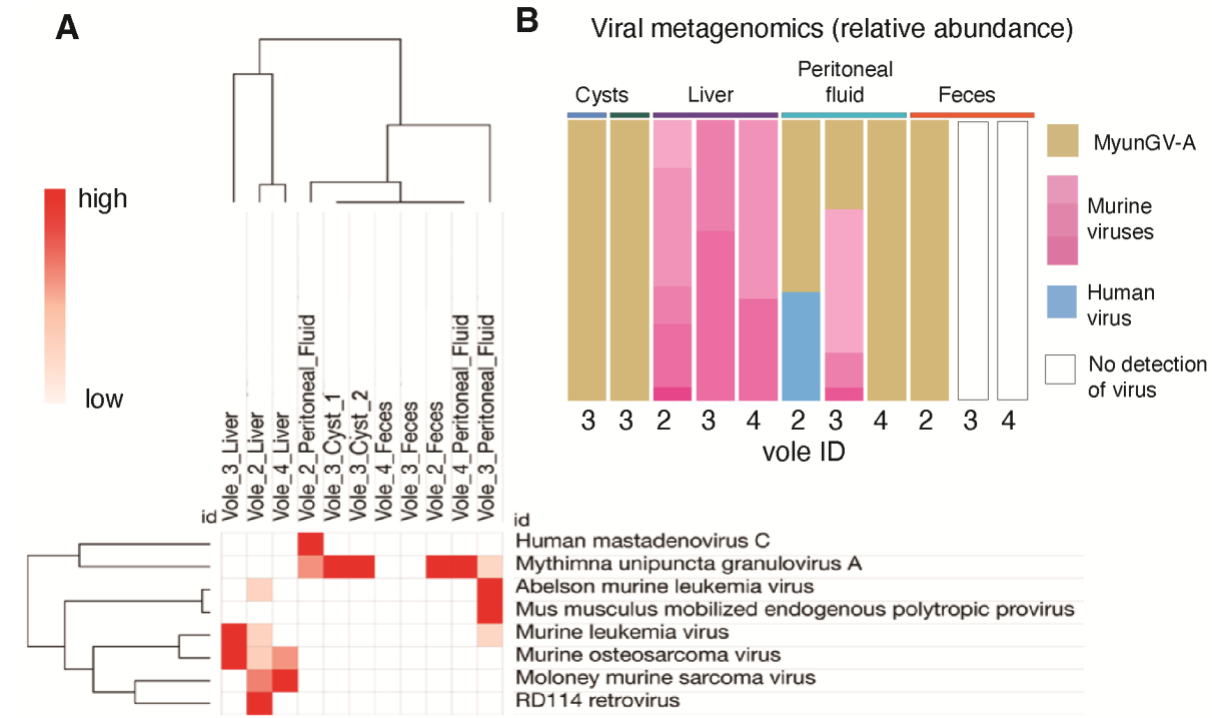


369  
370  
371  
372  
373  
374

**Figure 2. Metagenomic analysis identifies reproducible commensal *Bacteroidota* and opportunistic *Pseudomonadota* (*Enterobacteriaceae*) in the parasitic cysts. A)** Relative abundance across samples. **B)** Comparison of bacteria in both cysts demonstrates consistent pattern of abundance among similar bacteria, including *K. variicola*, *P. distasonis*, and *Bacteroidales*.

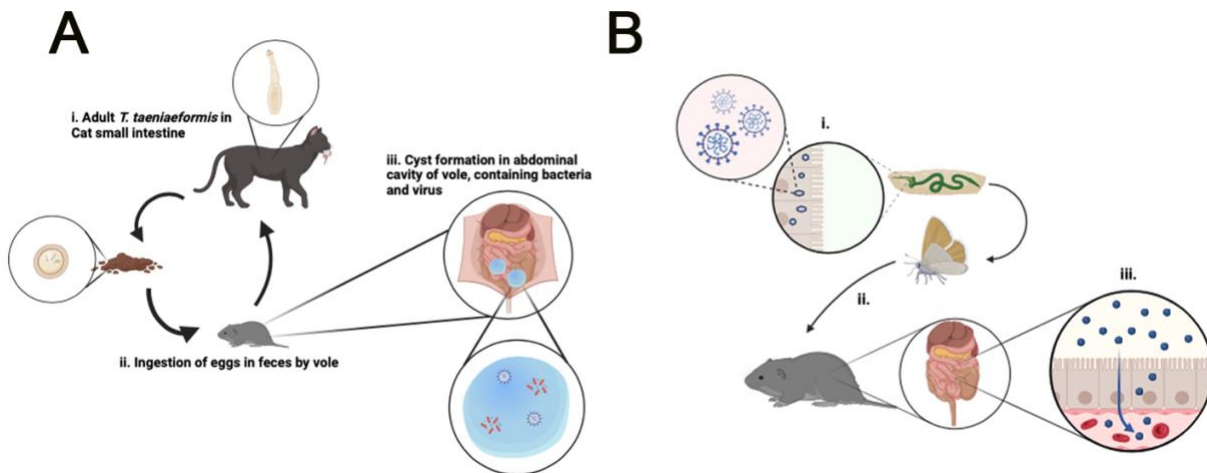
375

376



377

378 **Figure 3. Metagenomic analysis of viruses revealed MyunGV-A in Hydatygera larval cysts**  
379 **and peritoneal fluid of wild voles. A)** Hierarchical clustering of samples based on abundance.  
380 **B)** Abundance bar plot. MyunGV-A in both cysts was 100%, with similar  
381 findings in the peritoneal fluid and feces of two voles.



382

383 **Figure 4. Overview of *Hydatigera taeniaeformis* lifecycle and metacestode larval cystic stages**  
384 **in rodents and our theory of how MyunGV-A viral DNA could reach and co-adapt with**  
385 **bacteria in tapeworm cysts. A) Left panel. *H. taeniaeformis* responsible for cyst formation in**  
386 **the peritoneal cavity in rodents may serve as a conducive environment for the retention and**  
387 **replication of MyunGV-A and bacteria. The cysts may offer protection against external factors**  
388 **and create a microenvironment suitable for these microorganisms, facilitating evasion of the**  
389 **immune system. B) Right panel. Presumptive theory for acquisition of the insect virus by voles is**  
390 **presumed to have occurred indirectly through dietary sources e.g., ingestion of insects or**  
391 **vegetation carrying MyunGV-A contaminants. Steps in proposed cycle: i., MyunGV-A replicates**  
392 **in the midgut epithelial cells of armyworms; ii., vole consumes armyworm moth; iii., MyunGV-**  
393 **A is absorbed by via the brush border of the intestinal epithelial cells and into the bloodstream,**  
394 **disseminating to the cysts, or follows the *H. taeniaeformis* as it migrates through the gut wall to**  
395 **extra-intestinal tissues to start the cystic stage of the tapeworm.**

396 **References:**

- 397 1. Webster NS. Cooperation, communication, and co-evolution: grand challenges in microbial  
398 symbiosis research. *Front Microbiol.* 2014;5:164. doi:10.3389/fmicb.2014.00164
- 399 2. Raina JB, Eme L, Pollock FJ, Spang A, Archibald JM, Williams TA. Symbiosis in the  
400 microbial world: from ecology to genome evolution. *Biol Open.* Feb 22  
401 2018;7(2)doi:10.1242/bio.032524
- 402 3. Yeoman CJ, Chia N, Yildirim S, et al. Towards an Evolutionary Model of Animal-  
403 Associated Microbiomes. *Entropy.* 2011;13(3):570-594.
- 404 4. McFall-Ngai MJ. Giving microbes their due--animal life in a microbially dominant world. *J  
405 Exp Biol.* Jun 2015;218(Pt 12):1968-73. doi:10.1242/jeb.115121
- 406 5. Rodriguez-Palacios A, Kodani T, Kaydo L, et al. Stereomicroscopic 3D-pattern profiling of  
407 murine and human intestinal inflammation reveals unique structural phenotypes. *Nat  
408 Commun.* 2015;6:7577. doi:10.1038/ncomms8577
- 409 6. Yang F, Kumar A, Davenport KW, et al. Complete Genome Sequence of a Parabacteroides  
410 distasonis Strain (CavFT hAR46) Isolated from a Gut Wall-Cavitating Microlesion in a  
411 Patient with Severe Crohn's Disease. *Microbiol Resour Announc.* Sep  
412 2019;8(36)doi:10.1128/MRA.00585-19
- 413 7. Singh V, West G, Fiocchi C, et al. Clonal Parabacteroides from Gut Microfistulous Tracts as  
414 Transmissible Cytotoxic Succinate-Commensal Model of Crohn's Disease Complications.  
415 *bioRxiv.* Jan 10 2024;doi:10.1101/2024.01.09.574896
- 416 8. Bank NC, Vaidhvi S, Grubb B, et al. The basis of antigenic operon fragmentation in  
417 Bacteroidota and commensalism. *bioRxiv* 20230602543472; doi:  
418 <https://doi.org/10.1101/20230602543472>. 2023;
- 419 9. Singh V, Rodriguez-Palacios A. Genomes of Bacteroides ovatus, B. cellulosilyticus, B.  
420 uniformis, Phocaeicola vulgatus, and P. dorei isolated from Gut Cavernous Fistulous Tract  
421 Micropathologies in Crohn's disease. *MRA.* 2024;
- 422 10. Caira JN, Jensen K. Electron microscopy reveals novel external specialized organs housing  
423 bacteria in eagle ray tapeworms. *PLoS One.* 2021;16(1):e0244586.  
424 doi:10.1371/journal.pone.0244586
- 425 11. Bonelli P, Serra E, Dei Giudici S, et al. Molecular phylogenetic analysis of Echinococcus  
426 granulosus sensu lato infecting sheep in Italy. *Acta Trop.* Apr 2024;252:107151.  
427 doi:10.1016/j.actatropica.2024.107151
- 428 12. Romig T, Wassermann M. Echinococcus species in wildlife. *Int J Parasitol Parasites Wildl.*  
429 Apr 2024;23:100913. doi:10.1016/j.ijppaw.2024.100913
- 430 13. Celik F, Selcuk MA, Kilinc SG, et al. Molecular discrimination of G1 and G3 genotypes of  
431 Echinococcus granulosus sensu stricto obtained from human, cattle, and sheep using the  
432 mitochondrial NADH dehydrogenase subunit 5 marker. *Acta Trop.* Apr 2024;252:107124.  
433 doi:10.1016/j.actatropica.2024.107124

- 434 14. Casulli A, Pane S, Randi F, et al. Primary cerebral cystic echinococcosis in a child from  
435 Roman countryside: Source attribution and scoping review of cases from the literature. *PLoS*  
436 *Negl Trop Dis.* Sep 2023;17(9):e0011612. doi:10.1371/journal.pntd.0011612
- 437 15. Bao J, Zheng H, Wang Y, et al. *Echinococcus granulosus* Infection Results in an Increase in  
438 *Eisenbergiella* and *Parabacteroides* Genera in the Gut of Mice. *Front Microbiol.*  
439 2018;9:2890. doi:10.3389/fmicb.2018.02890
- 440 16. Browne HP, Forster SC, Anonye BO, et al. Culturing of 'unculturable' human microbiota  
441 reveals novel taxa and extensive sporulation. *Nature.* 05 2016;533(7604):543-546.  
442 doi:10.1038/nature17645
- 443 17. Szabó BG, Kiss R, Makra N, et al. Composition and changes of blood microbiota in adult  
444 patients with community-acquired sepsis: A. *Front Cell Infect Microbiol.* 2022;12:1067476.  
445 doi:10.3389/fcimb.2022.1067476
- 446 18. Thoendel M, Jeraldo P, Greenwood-Quaintance KE, et al. Comparison of Three Commercial  
447 Tools for Metagenomic Shotgun Sequencing Analysis. *J Clin Microbiol.* Feb 24  
448 2020;58(3)doi:10.1128/JCM.00981-19
- 449 19. CosmosID. Metagenomics Cloud, app.cosmosid.com, CosmosID Inc.,  
450 [www.cosmosid.com](http://www.cosmosid.com) 2024;
- 451 20. Yan Q, Wi YM, Thoendel MJ, et al. Evaluation of the CosmosID Bioinformatics Platform  
452 for Prosthetic Joint-Associated Sonicate Fluid Shotgun Metagenomic Data Analysis. *J Clin*  
453 *Microbiol.* Feb 2019;57(2)doi:10.1128/JCM.01182-18
- 454 21. Martin W. Linking causal concepts, study design, analysis and inference in support of one  
455 epidemiology for population health. *Preventive Veterinary Medicine.* 2008;86(3-4):270-288.
- 456 22. Rodriguez-Palacios A, Aladyshkina N, Ezeji JC, et al. 'Cyclical Bias' in Microbiome  
457 Research Revealed by A Portable Germ-Free Housing System Using Nested Isolation. *Sci*  
458 *Rep.* Feb 2018;8(1):3801. doi:10.1038/s41598-018-20742-1
- 459 23. Raffner Basson A, Gomez-Nguyen A, LaSalla A, et al. Replacing Animal Protein with Soy-  
460 Pea Protein in an "American Diet" Controls Murine Crohn Disease-Like Ileitis Regardless of  
461 Firmicutes: Bacteroidetes Ratio. *J Nutr.* 03 2021;151(3):579-590. doi:10.1093/jn/nxaa386
- 462 24. Basson AR, Gomez-Nguyen A, Menghini P, et al. Human Gut Microbiome Transplantation  
463 in Ileitis Prone Mice: A Tool for the Functional Characterization of the Microbiota in  
464 Inflammatory Bowel Disease Patients. *Inflamm Bowel Dis.* Feb 11 2020;26(3):347-359.  
465 doi:10.1093/ibd/izz242
- 466 25. Harrison RL, Mowery JD, Bauchan GR, Theilmann DA, Erlandson MA. The complete  
467 genome sequence of a second alphabaculovirus from the true armyworm, *Mythimna*  
468 *unipuncta*: implications for baculovirus phylogeny and host specificity. *Virus Genes.* Feb  
469 2019;55(1):104-116. doi:10.1007/s11262-018-1615-7
- 470 26. García M, Ortego F, Hernández-Crespo P, Farinós GP, Castañera P. Inheritance, fitness  
471 costs, incomplete resistance and feeding preferences in a laboratory-selected MON810-  
472 resistant strain of the true armyworm *Mythimna unipuncta*. *Pest Manag Sci.* Dec  
473 2015;71(12):1631-9. doi:10.1002/ps.3971

- 474 27. Gomez-Puerta LA, Vargas-Calla A, Garcia-Leandro M, et al. Identification of wild rodents  
475 as intermediate hosts for *Hydatigera taeniaeformis* in Peru. *Parasitol Res.* Aug  
476 2023;122(8):1915-1921. doi:10.1007/s00436-023-07892-6
- 477 28. Jia W, Yan H, Lou Z, et al. Mitochondrial genes and genomes support a cryptic species of  
478 tapeworm within *Taenia taeniaeformis*. *Acta Trop.* Sep 2012;123(3):154-63.  
479 doi:10.1016/j.actatropica.2012.04.006
- 480 29. Cook RW, Trapp AL, Williams JF. Pathology of *Taenia taeniaeformis* infection in the rat:  
481 hepatic, lymph node and thymic changes. *J Comp Pathol.* Apr 1981;91(2):219-26.  
482 doi:10.1016/0021-9975(81)90026-8
- 483 30. Mahesh Kumar J, Reddy PL, Aparna V, et al. *Strobilocercus fasciolaris* infection with  
484 hepatic sarcoma and gastroenteropathy in a Wistar colony. *Vet Parasitol.* Nov 05  
485 2006;141(3-4):362-7. doi:10.1016/j.vetpar.2006.05.029
- 486 31. Zhu M, Wang C, Yang S, et al. Alterations in Gut Microbiota Profiles of Mice Infected with  
487 *Echinococcus granulosus* sensu lato Microbiota Profiles of Mice Infected with *E. granulosus*  
488 s.l. *Acta Parasitol.* Dec 2022;67(4):1594-1602. doi:10.1007/s11686-022-00613-6
- 489 32. Cao D, Pang M, Wu D, et al. Alterations in the Gut Microbiota of Tibetan Patients With  
490 *Echinococcosis*. *Front Microbiol.* 2022;13:860909. doi:10.3389/fmicb.2022.860909
- 491 33. Liu Z, Yin B. Alterations in the Gut Microbial Composition and Diversity of Tibetan Sheep  
492 Infected With. *Front Vet Sci.* 2021;8:778789. doi:10.3389/fvets.2021.778789
- 493 34. Wu J, Zhu Y, Zhou L, et al. Parasite-Derived Excretory-Secretory Products Alleviate Gut  
494 Microbiota Dysbiosis and Improve Cognitive Impairment Induced by a High-Fat Diet. *Front  
495 Immunol.* 2021;12:710513. doi:10.3389/fimmu.2021.710513
- 496 35. Clem RJ, Passarelli AL. Baculoviruses: sophisticated pathogens of insects. *PLoS Pathog.*  
497 2013;9(11):e1003729. doi:10.1371/journal.ppat.1003729
- 498 36. Rohrmann GF. Baculovirus Molecular Biology. 2013.
- 499 37. Weldon L, Abolins S, Lenzi L, Bourne C, Riley EM, Viney M. The Gut Microbiota of Wild  
500 Mice. *PLoS One.* 2015;10(8):e0134643. doi:10.1371/journal.pone.0134643
- 501 38. Viney M. The gut microbiota of wild rodents: Challenges and opportunities. *Lab Anim.* Jun  
502 2019;53(3):252-258. doi:10.1177/0023677218787538
- 503 39. Li Y, Liu X, Tang P, Zhang H, Qin Q, Zhang Z. Genome sequence and organization of the  
504 *Mythimna* (formerly *Pseudaletia*) *unipuncta* granulovirus Hawaiian strain. *Sci Rep.* Jan 11  
505 2021;11(1):414. doi:10.1038/s41598-020-80117-3
- 506 40. Mukawa S, Goto C. In vivo characterization of two granuloviruses in larvae of *Mythimna*  
507 *separata* (Lepidoptera: Noctuidae). *J Gen Virol.* Apr 2008;89(Pt 4):915-921.  
508 doi:10.1099/vir.0.83365-0
- 509 41. Lacey LA, Grzywacz D, Shapiro-Ilan DI, Frutos R, Brownbridge M, Goettel MS. Insect  
510 pathogens as biological control agents: Back to the future. *J Invertebr Pathol.* Nov  
511 2015;132:1-41. doi:10.1016/j.jip.2015.07.009

- 512 42. van Oers MM, Pijlman GP, Vlak JM. Thirty years of baculovirus-insect cell protein  
513 expression: from dark horse to mainstream technology. *J Gen Virol*. Jan 2015;96(Pt 1):6-23.  
514 doi:10.1099/vir.0.067108-0
- 515 43. Zhang P, Zhang Y, Cao L, et al. A Diverse Virome Is Identified in Parasitic Flatworms of  
516 Domestic Animals in Xinjiang, China. *Microbiol Spectr*. Jun 15 2023;11(3):e0070223.  
517 doi:10.1128/spectrum.00702-23
- 518